High Temperatures-High Pressures, Vol. 46, pp. 321–332
Reprints available directly from the publisher
Photocopying permitted by license only

DC and AC scanning thermal microscopy using micro-thermoelectric probe†

ALEXIA BONTEMPI[1], LAURENT THIERY[1,*], DAMIEN TEYSSIEUX[1],
DANICK BRIAND[2] AND PASCAL VAIRAC[1]

[1]*Femto-St, CNRS UMR 6174, 32 Avenue de l'Observatoire,*
25044 Besançon Cedex, France
[2]*SAMLAB, Institute of Microengineering, Ecole Polytechnique Fédérale de Lausanne,*
Neuchâtel, Switzerland

Received: October 23, 2013. Accepted: February 22, 2014.

A scanning thermal microscope working in passive mode is described. This tool uses a thermocouple probe and is presented as a thermal imaging system. The surface temperature distribution of a thermal micro-component is presented. We point out the capacity of our system to perform surface temperature images under conditions for which most of usual techniques cannot operate. The thermal microscope is insensitive to optical surface parameters, can operate from ambient to 1000 K and allow measuring DC and AC temperature components.

Keywords: Scanning thermal microscope, micro-thermocouple, thermal imaging.

1 INTRODUCTION

Nowadays, the improvement of the local thermal characterization techniques remains challenging for a better understanding of energy transport at micro and nano-scales and expected developments in the field of novel materials. Thermal microscopes are generally used either to map the surface temperature of microsystems or the thermal conductivity of materials (derived from probe-to-sample thermal admittance). This defines passive or active mode of operation respectively. However, passive mode represents a larger class of available imaging systems that can be classified in two groups: conventional

*Corresponding author: laurent.thiery@univ-fcomte.fr
†This work has been presented to QMNTIA2013.

and near-field. Conventional are generally non-contact techniques which are noninvasive methods but highly depending on the surface optical nature. They are also restricted in terms of temperature range and spatial resolution due to Rayleigh criterion. Depending on the wavelength range, standard infrared techniques are limited to several micrometers whereas near-infrared thermography which operates above 500 K exhibits a spatial resolution near 500 nm [1,2], Thermoreflectance [3–5], photoluminescence [6] or Raman spectroscopy [7,8] techniques are extremely sensitive to the surface nature (optical characteristics, roughness) and their spatial resolution remains limited to about one micrometer. Furthermore, these methods are also limited in terms of temperature range to several tens of degrees above ambient. Near-field techniques are based on a local interaction between a probe tip and the sample surface. Lateral resolution results from the tip-to-surface interaction area which depends on its physical nature. The specific case of a thermal interaction remains unclearly defined even if it is roughly related to the tip dimension. This is the case for liquid crystal thermography [9], fluorescence thermography [10] or near-field optical thermography (NFOT) [11]. Stemming from far-field techniques, these optical methods have joined the Scanning Thermal Microscopy (SThM) imaging systems derived from the principle of the Scanning Tunneling Microscope (STM) in 1986. Among the most wide-spread near-field probes, two main families can be distinguished; thermoresistive probes for which the temperature is deduced from its mean sensitive part value (micro-wire or thin film) [12,13] and thermocouple (or thermodiode) probes that provide a quasi-punctual temperature value [14,15]. Unfortunately, thermal diffusion between the tip and the sample occurs and must be taken in consideration for correcting the resulting contact temperature. Moreover, the highest measurable temperature remains lower than 750 K due to thermo-mechanical constraints that deform or damage the tip apex. We present results obtained by means of a bifilar thermocouple probe fabricated with a sparking technique [16]. Platinum and platinum-rhodium Wollaston wires of 1.3 μm in diameter are used.

2 EXPERIMENTAL SET-UP

2.1 Scanning and data acquisition principles

The homemade scanning thermal microscope principle is depicted in Figure 1. Three manual axes are used to position the sample relatively to the thermocouple probe. Smaract piezo-actuators (SLC 1730), are used in X and Y horizontal directions for long range and high accurate displacements of sample. A PI Mercury (M-231 and its controller C-863) system are used for the vertical positioning of the probe.

A point-to-point scan is performed to obtain a temperature mapping of the sample surface. The horizontal positioning of the device (x and y) and the

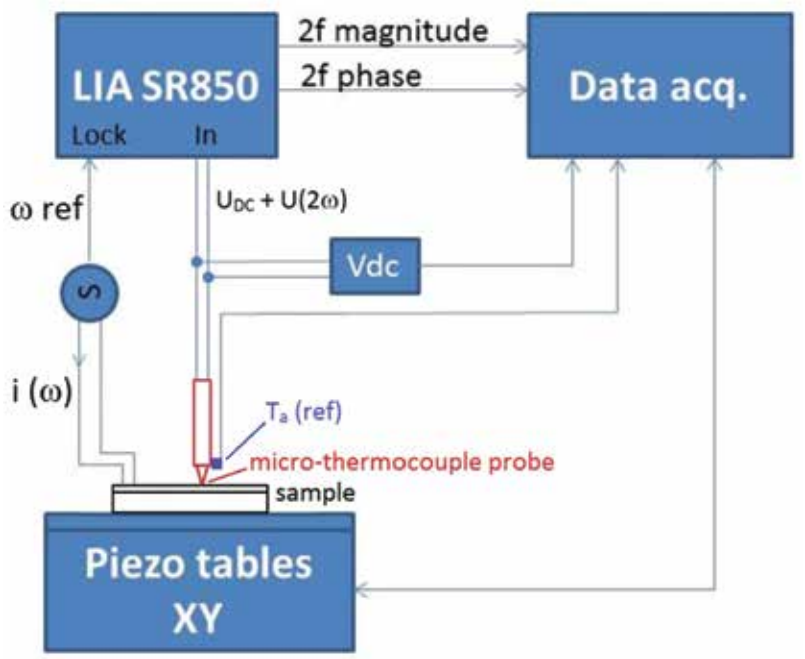

FIGURE 1
Experimental setup with the thermocouple probe.

vertical probe location (z) regarding to the sample are managed and recorded by a computer. Depending on excitation mode of the sample, several temperature components are available. When the device is supplied with an AC current, a double frequency (2f) temperature signal is extracted by a lock-in amplifier. A DC component is measured by a low pass filter voltmeter which gives the static temperature value after correcting the cold junction by means of the ambient temperature extracted from a resistive platinum sensor (Pt1000) located in the vicinity of the probe tip. Since the thermal equilibrium between the probe tip and the surface sample must be reached for each point, our system requires a larger time constant regarding to usual point by point imagers. This represents approximately one second even if the time constant of the thermocouple is much lower. More generally, measurements are possible only when the probe-sample-environment system thermal equilibrium is reached.

2.2 Microthermocouple probe

Since the coming of the SThM, various thermocouple probes have been developed. Some of them are micro-fabricated by means of a thin-film deposition on micropipette [17], on AFM cantilever [18,19] or on optical fiber

[20], others are welded by a sparking method to obtain a K type [21] or a S type sensor [22,23]. We have applied the last technique to perform S type micro-thermocouples using Wollaston wires of platinum and platinum-rhodium (90%–10%). In a first step, the silver cladding which covers the thin platinum (or platinum rhodium) wire is etched away by a chemical attack to expose the core. Platinum and platinum-rhodium wires are then welded using a capacitor discharge so as to obtain a V-shape as shown in Figure 2. The junction thermoelectric voltage is converted in temperature using standard S type conversion law. The Seebeck coefficient, depending on the temperature value, is $5.88\,\mu V\ K^{-1}$ at 20°C, $9.13\,\mu V\ K^{-1}$ at 300°C and $10.87\,\mu V\ K^{-1}$ at 800°C in accordance with IEC 584-1 international standard. Reference temperature (cold junction) corresponds to the silver core area which behaves like a heat sink at ambient temperature. This was verified by means of a second microthermocouple moved along these silver wires. This is due to their length, their location regarding to the small hot surface (platinum and platinum-rhodium wires are about $300\,\mu m$ long) and their high thermal conductivity.

Prior any measurement in harmonic mode, we have checked the harmonic thermal pass-band of the probe. The thermocouple is supplied with an AC current at frequency f, generating a 2f heating source whose effect can be measured either at the 2f frequency (Seebeck voltage) or at the 3f frequency. The measurable 3f voltage is due to the temperature dependence of the wire resistance (2f) multiplied by the current (f). This component, taking account of the overall wire thermal inertia, is presented in Figure 3. The thermal cut-off frequency of the probe near 300 Hz corresponds to the frequency for which the magnitude decreases by a factor $\sqrt{2}$. As a consequence, AC temperature measurements are accurate if the thermal cut-off frequency of the tested device remains lower than 300 Hz.

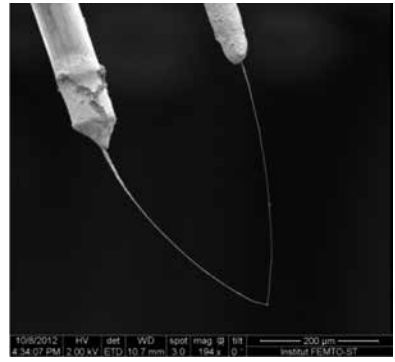

FIGURE 2
Thermocouple junction welded by the sparking method of capacitor discharge.

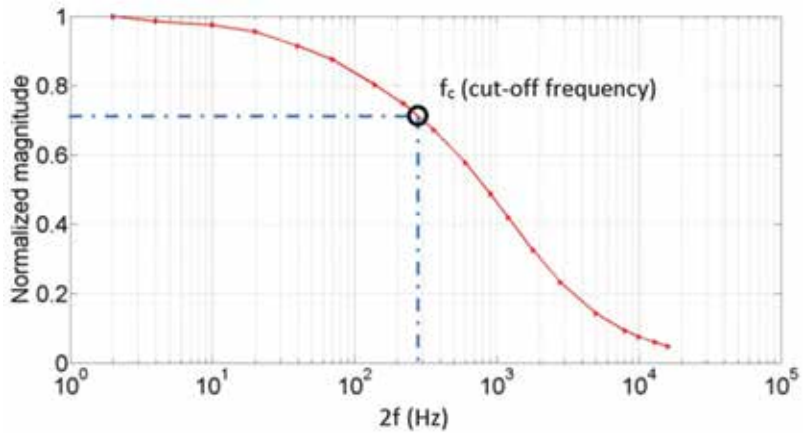

FIGURE 3
Frequency analysis of the probe thermoelectric voltage.

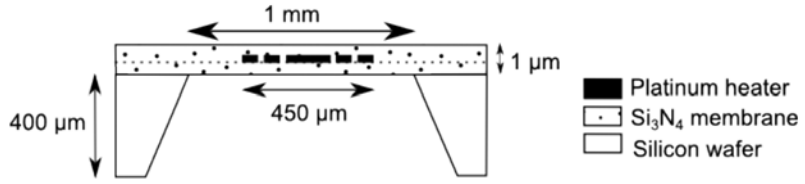

FIGURE 4
Micro-hotplate cross-section.

2.3 Sample design

The tested device is a micro-hotplate which was developed at the Institute of Microengineering of Neuchâtel (SAMLAB) and has been previously described in the reference [24]. A membrane of silicon nitride with 1 µm thick is suspended over a silicon substrate. A platinum coil heater of 200 nm thick is embedded in the membrane as shown in Figure 4. The key point of such a device is the possibility to generate a thermally homogeneous area at the center of the membrane by adjusting the bias current into the platinum heater. After having released the silicon substrate beneath the central area, the embedded coil is thermally isolated from the chip structure, so that its central temperature can exceed 1000 K for only a tenth of watt of consumption (see Figure 8).

An upside view of this micro-hotplate is shown in the Figure 5. Figure 5a presents an optical micrograph which highlights the specific design of the platinum heater, ensuring a homogenous temperature distribution. The coil is optically visible since silicon nitride is transparent in the visible to close infrared wavelength range. Consequently, this is a typical case for which

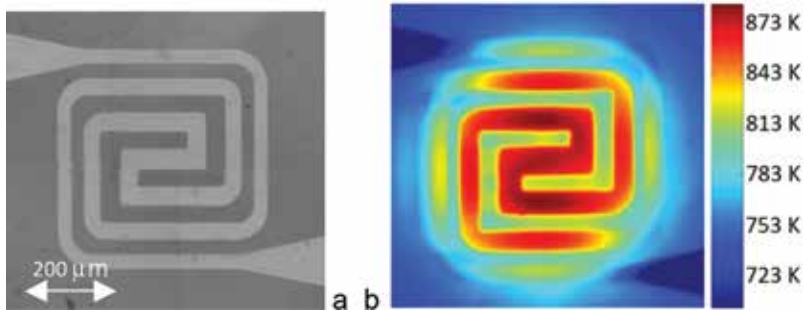

FIGURE 5
Optical upside view of the micro-heater (a). Near-infrared thermal image (b) at 75 mW DC supplied power.

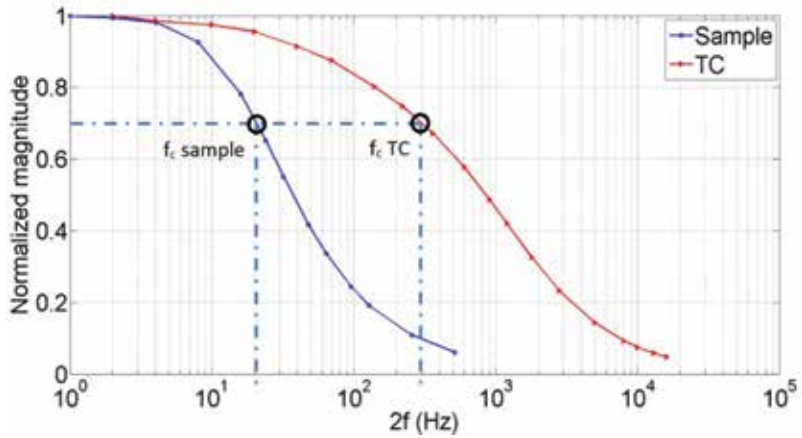

FIGURE 6
Frequency analysis of the thermal response of the micro-heater (sample) and the thermocouple probe (TC).

optical thermography techniques cannot operate for measuring surface temperature. Figure 5b gives a thermographic image of the same area obtained by means of near-infrared thermal microscope [1]. Only the embedded platinum heater appears whereas membrane surface temperature remains thermally invisible. Moreover, such a technique is not available for temperature range lower than 500 K typically and remains difficult for extracting harmonic components.

Figure 6 presents a comparison between the micro-hotplate and the thermocouple sensor thermal pass-band while supplying to them an AC current and extracting the 3f voltage. The thermal cut-off frequency of the micro-heater and the thermocouple probe is near 20 Hz and 300 Hz respectively.

Consequently, the thermocouple is able to measure periodic surface temperature if the supplied current frequency remains in the micro-heater thermal bandwidth.

3 RESULTS

3.1 Temperature measurement

Prior any measurement, the influence of the tip to surface contact force has to be specified. Indeed, the need of a feedback loop would complicate the imaging system and slow down the acquisition time. Figure 7 depicts the results of temperature measurements obtained for different contact forces on the membrane. Negative abscissa z corresponds to the distance between the thermocouple junction and the surface; $z = 0$ represents the contact point (dotted red line), and positive abscissa corresponds to an increase of the contact force up to 500 nN approximately ($z = 1\ \mu m$). The contact force cannot be measured with our set-up but estimated by a simple calculation based on the junction V-shape observed deformation. Once the contact occurs, the thermocouple signal is rather stabilized. This corresponds to a saturation of the thermal contact. Error bars represent standard deviation after 1000 recorded cycles of approaches. In the following results, and

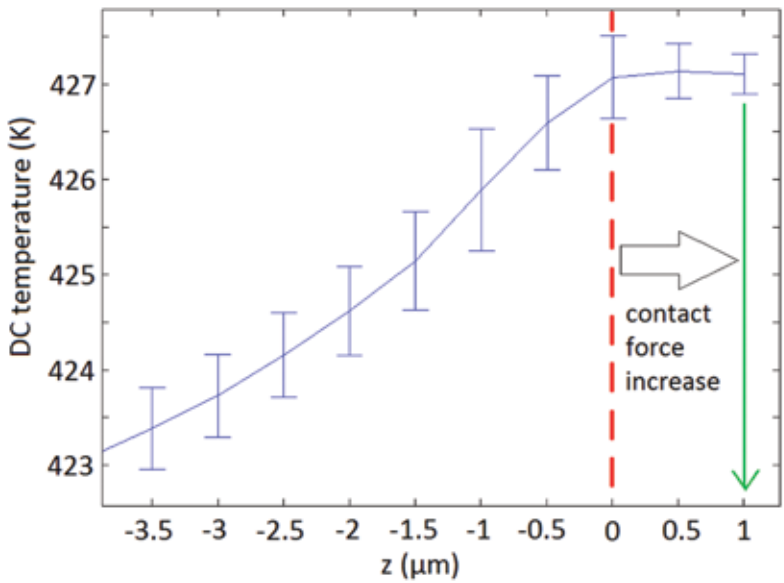

FIGURE 7
Temperature measurements versus the tip to sample distance above the central point of the micro-hotplate and the effect of the contact force increase (12 mW DC supplied power).

since the sample is flat, the position of the tip is defined from a reference plan previously acquired. In the following results, each temperature value is stored when the z position of the thermocouple junction is 1 µm (green arrow of Figure 7).

Before considering that measurements are reliable, the most important point to be considered is the effect of cooling down the surface due to heat transfer between the cold tip and the hot surface. We have performed and described the contact calibration procedure between the tip and this kind of micro-hotplate in reference [25], leading to a correction of the probe temperature using a calibration parameter τ called "thermal response" of the probe. Its value has been quantified after a thorough analysis of the heat transfer through the contact area. A mean value of 0.92 was extracted for this study. This characterizes the temperature correction of the used thermocouple probe associated to this particular sample in the present temperature range, such as:

$$T_s = \frac{T_p - T_a}{\tau} + T_a$$

In this expression, T_a, T_p and T_s are ambient, probe and surface (actual) temperatures respectively.

Figure 8 presents values of corrected surface temperature performed by contact on the central point of the micro-hotplate membrane versus its supplied power. This also demonstrates that the measurement range of a micro-thermocouple probe can exceed 1000 K typically.

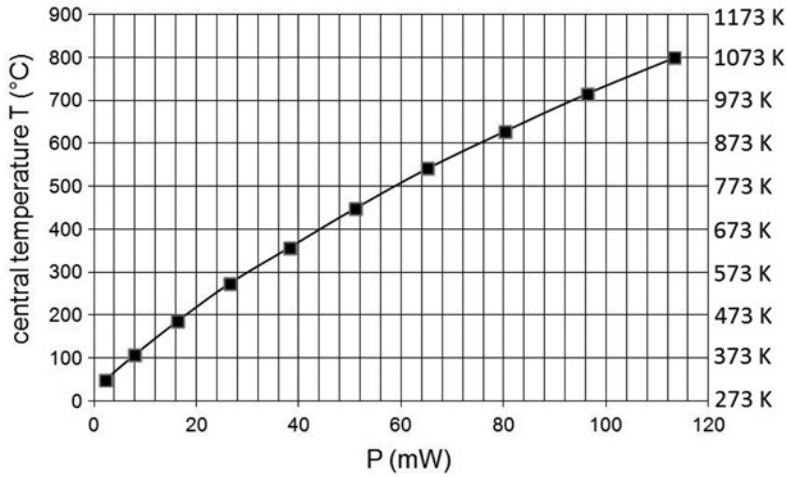

FIGURE 8
Central temperature measured by the thermocouple probe up to 800°C versus micro-hotplate supplied power.

3.2 Temperature mapping

As introduced in section 2, the micro-hotplate is supplied with an AC current that generates by Joule effect both AC at double frequency 2f and DC heating. DC voltage is converted following the Seebeck response of the S type standard law, corrected from ambient temperature (cold junction). The AC RMS 2f voltage is converted in temperature according to the Seebeck coefficient at the DC temperature value. A point by point contact measurement scan provides three simultaneous images of DC, AC magnitude and AC phase of the temperature components. Changing the current frequency allows to reveal different thermal contrasts. An example of surface temperature images is presented in Figure 9. The complete membrane is 1 mm square but the scan is performed on its central area which represents a square of $560 \times 560\,\mu m^2$. An optical view (Figure 9a) clearly shows the platinum coil (heater) because of the transparency of the silicon nitride membrane. The supplied AC current value is 12 mA RMS at a frequency of 270 Hz. DC temperature image (Figure 9b) clearly shows the thermal homogeneity of the central area whereas AC 2f components reveal interesting thermal contrasts both in phase (Figure 9c) and magnitude (Figure 9d).

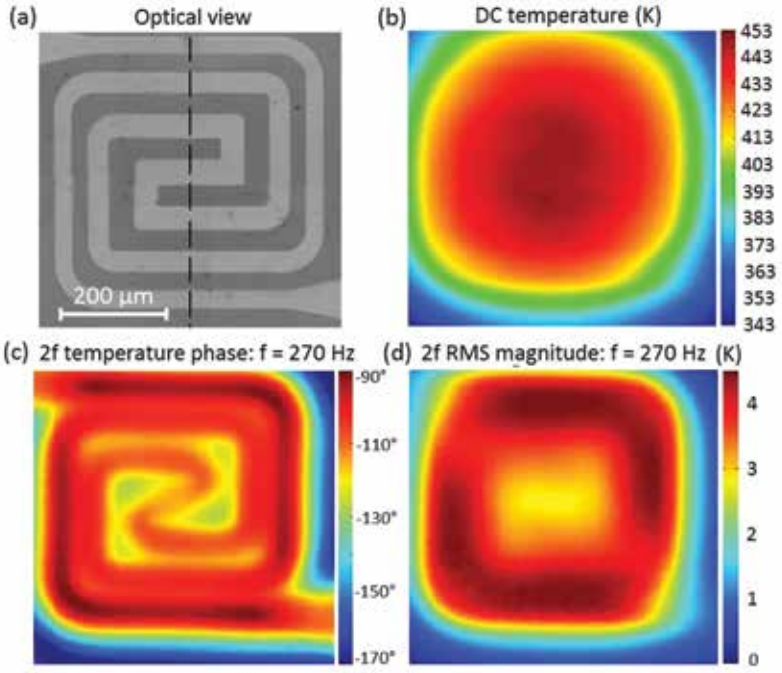

FIGURE 9
AC and DC temperature images of the micro-heater area ($560 \times 560\,\mu m^2$), supplied by an AC current at the frequency f = 270 Hz.

The measured phase signal corresponds to a lag between the supply current at frequency f and the extracted 2f signal, revealing the thermal diffusion effect into the material whereas the AC temperature magnitude points out the heat source intensity. Without surprise, the latter is more important in the thinner portion of the coil which exhibits higher electrical resistance. Besides, the influence of the current frequency helps to reveal these details as presented in Figure 10 while the sensor is scanned following a line (dotted black line of Figure 9a).

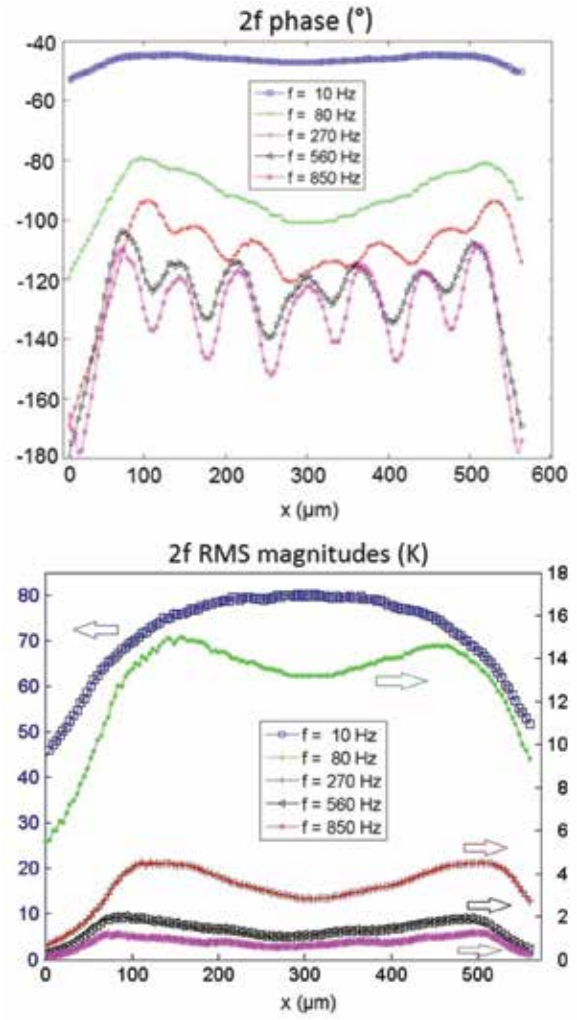

FIGURE 10
Profiles of phase and magnitude AC temperature at different frequencies. Measurement points correspond to dashed line of Figure 9a.

The phase contrast classically increases with the frequency and the magnitude decreases due to the thermal pass band of both sample and probe. Phase is depending on the material so that its value remains high in the heater whereas it decreases linearly into the passive material (membrane). Further quantitative data could be extracted in this area such as the thermal diffusivity which is related to the phase slope for a given frequency. Indeed, if the chosen frequency is high enough, typically above some hundreds of Hz, the linear portions of phase slopes of Figure 10 are given by the ratio $\sqrt{\omega/a}$ where a is the thermal diffusivity ($m^2 s^{-1}$) and $\omega = 2\pi f_{th}$ is the pulsation of the thermal frequency f_{th} which corresponds to the double of the current frequency f. The extraction of thermal diffusivity from 270, 560 and 850 Hz phase slopes leads to a mean value of 6.9 10^{-6} m^2 s^{-1}.

4 CONCLUSION

We have presented a simple system of temperature imaging based on the use of a micro-thermocouple probe. Its main advantages rely on its insensitivity to surface optical nature and the possibility to operate from ambient to 1000 K. DC and AC measurements are reliable since a calibration procedure has been previously performed. This is an important point which was presented and discussed in a previous paper [25]. In spite of such a constraint and the acquisition time near one second per measured value typically, we consider the use of a micro-thermocouple as an alternative to usual thermography. The lateral resolution, generally related to the probe tip dimension, remains an open question in which sample nature and environment conditions (ambient or vacuum) have to be taken in consideration. Furthermore, the contact area related to the applied force, the sample and probe materials and eventually the surface relief are important points to be addressed. These are further objectives since the present system will be improved to operate in active mode for sample thermal conductivity imaging by using 2 omega method and for which the contact force between the probe and the sample must be controlled [26].

REFERENCES

[1] D. Teyssieux, L. Thiery and B. Cretin, Rev. Sci. Instrum. 78, (2007) 034902.
[2] D. Teyssieux, D. Briand, J. Charnay, N. F. de Rooij and B. Cretin, J. Micromech. Micro-Eng. 18, (2008) 065005.
[3] J. Christofferson and A. Shakouri, Rev. Sci. Instrum. 76, (2005) 024903.
[4] G. Tessier, S. Holé, and D. Fournier, Appl. Phys. Lett. 78, (2001) 2267.
[5] I. A. Vitkin, C. Christofides, and A. Mandelis, J. Appl. Phys. 67, (1990) 2822.
[6] C. Herzum, C. Boit, J. Kölzer, J. Otto and R. Weiland, Microelectron. J. 29, (1998) 163–170.
[7] Kuball M., Rajasingam S., Sarua A., Uren M. J., Martin T., Hughes B. T., Hilton K. P. and R. S. Balmer, *Appl. Phys. Lett.* 82, (2003)124–126.

[8] A. Soudi, R. D. Dawson and Y. Gu, ACS Nano 5(1), (2011) 255–262.
[9] A. Csendes, V. Szekely and M. Rencz, Microelec. Engin. 31, (1996) 281–290.
[10] E. Saidi, B. Samson, L. Aigouy, S. Volz, P. Löw, C. Bergaud and M. Mortier, Nanotechnology 20, (2009) 115703.
[11] K. E. Goodson and M. Asheghi, Microscale Thermophys. Eng. 1, (1997) 225–235.
[12] R. B. Dinwiddie, R. J. Pyllki, P. E. West, Thermal Conductivity, edited by T. W. Tong (Technomics, Lancaster, PA, 1994), Vol. 22, p. 668.
[13] G. Mills, J. M. R. Weaver, G. Harris, W. Chen, J. Carrejo, L. Johnson and B. Rogers, U*ltramicroscopy* 80(1), (1999) 7–11.
[14] G. Mills, H. Zhou, A. Midha, L. Donaldson and J. M. R. Weaver, Appl. Phys. Lett. 72(22), (1998) 2900–2902.
[15] L. Shi, O. Kwon, A. C. Miner and A. Majumdar, J. MicroElectroMech. Sys. 10(3), (2001) 370–378.
[16] P. Voisin, L. Thiery and G. Bröm, Eur. Phys. J. Appl. Phys. 7(2), (1999) 177–187.
[17] G. Fish, O. Bouevitch, S. Kolotov, K. Lieberman, D. Palanker, I. Turovets and A. Lewis, Rev. Sci. Instrum. 66(5), (1995) 3300–3306.
[18] Yo. Zhang, Ya. Zhang, J. Blaser, T. S. Sriram, A. Enver and R.B. Marcus, Rev. Sci. Instrum. 69(5), (1998) 2081–2084.
[19] T. Leinhos, M. Stopka, E. Oesterschulze, Appl. Phys. A 66, (1998) S65.
[20] L. Thiery, C. Bainier and M. Spajer, *OPTO 2002 International Conference Proceedings, 14–16 May 2002, Erfurt, Germany* (AMA Service GmbH, 2002), pp. 193–196.
[21] A. Majumdar, J. Lai, M. Chandrachood, O. Nakabeppu, Y. Wu and Z. Shi, Rev. Sci. Instrum. 66(6), (1995) 3584–3592.
[22] R. A. Secco and R. F. Tucker, Rev. Sci. Instrum. 63(11), (1992) 5485–5486.
[23] L. Thiery, Rev. Gen. Therm. n°394, (1994) 551–561.
[24] D. Briand, S. Colin, A. Gangadharaiah, E. Vela, P. Dubois, L. Thiery and N. F. De Rooij, *Sensors and Actuators* A 132 (2006) 317–324.
[25] L. Thiery, S. Toullier, D. Teyssieux, D. Briand, J. Heat Transfer 130, (2008) 091601.
[26] L. Thiery, E. Gavignet and B. Cretin, *Rev. Sci. Instrum.* 80, (2009) 034901.